Observations on Probabilistic Slope Stability Analysis

D.V. Griffiths[1,3], Desheng Zhu[2], Jinsong Huang[3] and Gordon A. Fenton[4]

[1]*Colorado School of Mines. Email: d.v.griffiths@mines.edu*
[2]*Hohai University. Email: zhudesheng87@163.com*
[3]*University of Newcastle. Email: jinsong.huang@newcastle.edu.au*
[4]*Dalhousie University. Email: Gordon.fenton@dal.ca*

Abstract: The paper reflects on developments and advances in probabilistic slope stability analysis, particularly when soil properties are modeled using random field theory in conjunction with elastic-plastic finite element analysis. Discussion will include the "seeking out" effect of failure mechanisms, "worst case" spatial correlation lengths, and some examples of slopes with linearly increasing mean strength. It is suggested that numerical discretization approaches to probabilistic slope stability represent the most rational way forward, and use of classical limit equilibrium slope stability methods with fixed failure mechanisms should be avoided.

Keywords: probabilistic slope stability, random fields, finite elements

1. Introduction

Slope stability analysis is a branch of geotechnical engineering that is highly amenable to probabilistic treatment, and has received considerable attention in the literature. Important early probabilistic papers appeared in the 1970s (e.g., Lumb 1970, 1972; Matsuo and Kuroda 1974; Alonso 1976; Tang et al. 1976; Vanmarcke 1977a, 1977b; Yong et al. 1977) and publications have continued at an ever increasing rate. According to the SCOPUS citation database, the most cited papers on probabilistic soil slope stability analysis (excluding those specifically on rock slopes, earthquakes or landslides) include: Vanmarcke (1977a), Christian et al. (1994), Griffiths and Fenton (2004), Whitman (1984), EI-Ramly et al. (2002), Li and Lumb (1987), Vanmarcke (1977b), Wong (1985), Hassan and Wolff (1999), Husein Malkawi et al. (2000), Griffiths et al. (2009), Alonso (1976), Low et al. (1998), Tang et al. (1976). Baecher and Christian (2003) published the first textbook dedicated to geotechnical reliability, and important contributions, especially in the realm of engineering practice, should be mentioned from Duncan (2000), the NGI group (e.g., Lacasse 1994; Lacasse and Nadim 1996; Uzielli et al. 2008; Lacasse et al. 2004, 2007, 2013a, 2013b) and the University of New South Wales (e.g.,

Lee et al. 1983; Mostyn and Soo 1992; Mostyn and Li 1993).

Lacasse et al. (2013a) discussed some geotechnical projects benefiting from probabilistic approaches, but also noted that the geotechnical profession was slow to adopt these methods in geotechnical design, especially in traditional problems such as slopes and foundations.

In his foreword to the inaugural issue of *Géotechnique* in 1948, Karl Terzaghi wrote, *"...in earthwork engineering the designer has to deal with bodies of earth with a complex structure and the properties of the material may vary from point to point."*

While tools have been developed for tackling probabilistic geotechnical analysis, ranging from event trees to first order second moment (FOSM) and first order reliability methods (FORM) (e.g., Whitman 1984; Wolff 1996; Lacasse 1994; Christian et al. 1994; Hassan and Wolff 1999; Duncan 2000), the role of spatial variability referred to in Terzaghi's preface is regularly ignored, even though its importance in slope stability analysis has long been recognized (e.g., Mostyn and Soo 1992).

Griffiths and Fenton (2004) and Griffiths et al. (2009) showed that simplified probabilistic analyses, in which spatial variability is ignored (by essentially assuming infinite correlation lengths), can lead to unconservative estimates of

the probability of failure. Furthermore, it has also been observed that some probabilistic geotechnical analyses display a "worst case" spatial correlation length at intermediate scales, where the probability of failure is a maximum.

At the time of writing, the majority of probabilistic slope stability analyses continue to combine probabilistic theories with classical limit equilibrium methods, often restricting failure surfaces to be circular. Spatial variability means that potential failure surfaces are frequently non-circular, as the mechanism "seeks out" the weakest path through the soil. In these circumstances, the assumption of a circular failure surface is liable to miss the important influence of spatial variability on failure, and lead to upper-bound solutions.

It is only quite recently that Terzaghi's observation of spatially varying soil properties was tackled explicitly by a numerical method called the Random Finite Element Method (RFEM), initially applied to seepage problems (Griffiths and Fenton 1993, Fenton and Griffiths 1993), and later to slope stability analysis (Griffiths and Fenton 2000, 2004; Hicks and Samy 2002, Fenton et al. 2003). In this work, slope stability analyses were presented using elastic-plastic finite elements combined with random fields. The random fields were generated using the Local Averaging Subdivision (LAS) method (Fenton and Vanmarcke 1990) which is able to model spatial variability while properly accounting for local averaging over each finite element. The deliverable in such an analysis by RFEM is the *probability of failure* as opposed to the classical *factor of safety*. Since the development of the RFEM in the mid-1990s, and the subsequent wide dissemination of the theory and programs (Fenton and Griffiths 2008) (e.g., http://inside.mines.edu/~vgriffit/rfem/) the method is now used by research groups worldwide and has become the state-of-the-art in advanced probabilistic geotechnical analysis.

Some of the issues relating to the proper modelling of spatial variability will be reviewed and discussed in this paper.

2. Seeking out Failure
2.1 Deterministic slope stability analysis
The use of finite elements as a deterministic method of slope stability analysis is now widely accepted (Griffiths and Lane 1999) and has been incorporated into several well-known commercial codes.

While circular failure surfaces are often adequate for homogeneous slopes, or slopes with gradually varying properties, the "seeking out" effect is easily demonstrated in layered soils. Fig. 1 shows a finite element analysis of the James Bay Dyke (e.g., Christian et al. 1994) clearly showing a non-circular critical failure surface passing through the weak soil below the dyke giving a factor of safety of $FS \approx 1.27$.
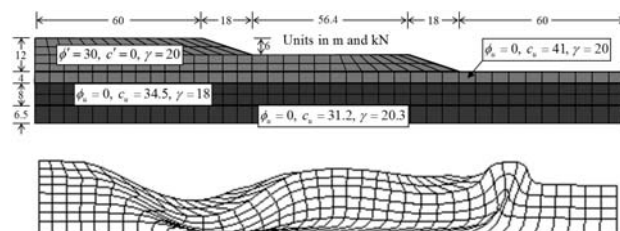
Figure 1. FE analysis of the James Bay Dyke

Another deterministic case where the benefits of finite element slope stability analysis are demonstrated is shown in Fig. 2, involving the analysis of a 3-layer slope.
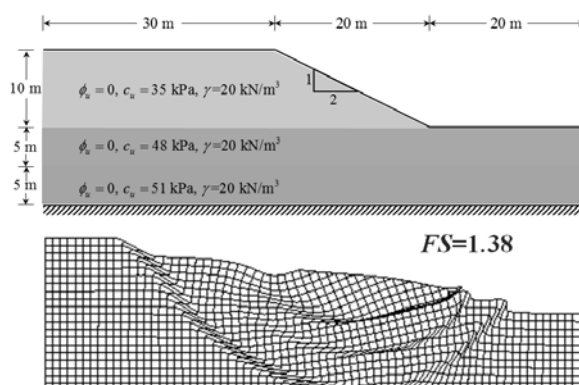
Figure 2. FE analysis of a 3-layer clay slope

In this case, the finite element analysis naturally detects three potential failure surfaces, all with about the same factor of safety of $FS \approx 1.38$. A conventional limit equilibrium analysis could easily have missed one or more of these failure surfaces.

The "seeking out" phenomenon is even more important when performing probabilistic studies using the RFEM.

2.2 Random slopes with linearly increasing strength with depth

Consider the case shown in Fig. 3 involving a lognormally distributed undrained slope with a linearly increasing mean strength and constant coefficient of variation (e.g., Griffiths et al. 2015).
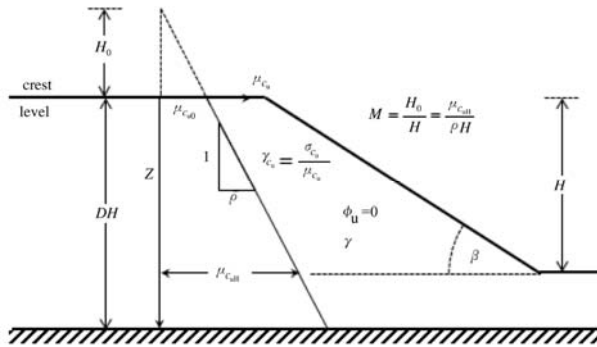
Figure 3. Random slope with linearly increasing mean strength

Normally consolidated soils regularly display an increasing undrained strength with depth due to the influence of the effective overburden pressure. A special case where the strength at the ground surface is zero ($\mu_{c_{u0}} = 0$) is sometimes referred to as a "Gibson soil" (Gibson and Morgenstern 1962).

With reference to Fig. 3 let the mean strength at $z = H$ be given as $\mu_{c_{uH}}$. In order to generate a random field with the properties

$$\begin{cases} \mu_{c_{uz}} = \mu_{c_{uH}} - \rho(H - z) \\ \sigma_{c_{uz}} = v_{c_u}\mu_{c_{uz}} \end{cases} \quad (1)$$

where $\mu_{c_{uz}} \geq 0$ and $0 \leq \rho \leq \dfrac{\mu_{c_{uH}}}{H}$.

Step 1:

Generate a homogeneous stationary lognormal random field based on the parameters at the base of the slope, i.e. mean $\mu_{c_{uH}}$, standard deviation $\sigma_{c_{uH}}$ and spatial correlation length θ. Let the initial values assigned to all elements at

this stage be c_{0i}, $i = 1, 2, \ldots, n$ where n is the number of elements in the mesh.

Step 2:

Element values are then adjusted to account for other depths using the scaling factor

$$c_{zi} = c_{0i}\frac{\mu_{c_{uH}} - \rho(H - z)}{\mu_{c_{uH}}}, \quad i = 1, 2, \ldots, n \quad (2)$$

where z is sampled at the centroid of each element. See the Appendix for more details.

It may be noted that for the special case where $\mu_{c_{uH}} = \rho H$, $\mu_{c_{u0}} = 0$, and Eq. (2) simplifies to

$$c_{zi} = c_{0i}\frac{z}{H}, \quad i = 1, 2, \ldots, n \quad (3)$$

It may also be noted that if $\rho = 0$, no adjustment is necessary, and the stationary random field generated in Step 1 is retained.

Fig. 4 shows two failure mechanisms from a suite of Monte-Carlo simulations on a slope with the properties indicated in the figure caption.
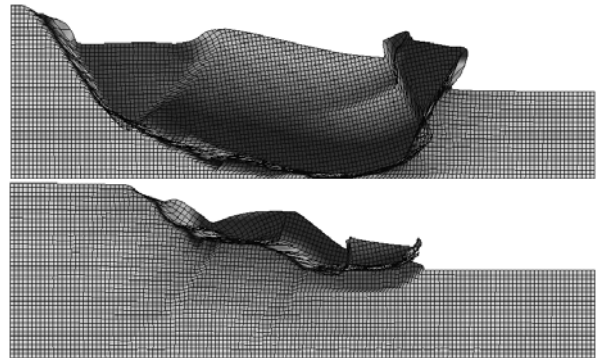
Figure 4. Failure simulations for a random slope with $\beta = 20°$, $M = 0.75$, $D = 1.5$, $v_{c_u} = 0.5$, $\Theta = 0.6$

An isotropic spatial correlation length $\Theta = \theta/H$ was assumed. The figures show complex critical failure mechanisms that are clearly non-circular, and which would defy meaningful analysis by any traditional limit equilibrium method.

Recent work on the deterministic slope stability problem shown in Fig. 3 (Griffiths and Yu 2015) has led to some modifications to the charts of Hunter and Schuster (1968). The

fundamental solution is a stability number N given by

$$N = f(\beta, D, M) \qquad (4)$$

after which the factor of safety can be retrieved as

$$FS = N\frac{r}{g} \qquad (5)$$

It may be noted that when $M = 0$ the stability number no longer depends on D, and is a function of β only, thus

$$N = f(\beta) \qquad (6)$$

A typical chart from Griffiths and Yu (2015) for the case of $M = 2$ is shown in Fig. 5. A striking characteristic of these charts is that as D increases, there comes a point where N no longer depends on D as indicated by the horizontal lines.

Considering the case of $\beta = 15°$, it can be seen that N falls quite steeply in the range $1 < D < 2$, but reaches a constant of $N \approx 23$ for all $D > 2$. Since $FS \propto N$ from Eq. (5), the same trend is true of the factor of safety.
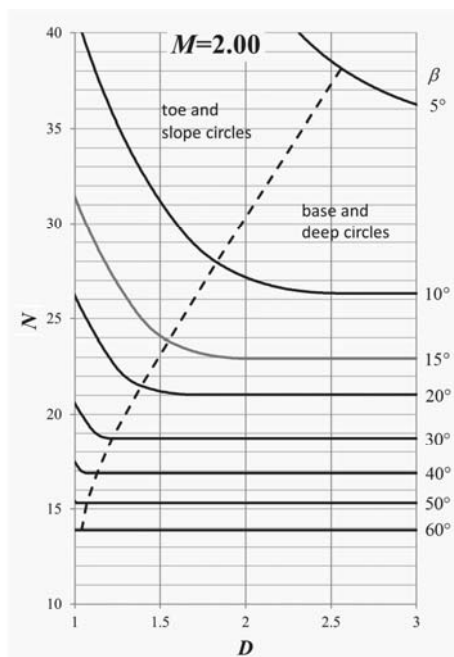
Figure 5. Deterministically, the stability number remains constant for $D>2$ when $\beta = 15°$ and $M = 2$ (see also Fig. 3)

A probabilistic analysis was performed on the same slope with $M = 2$ using RFEM assuming a random soil with linearly increasing mean strength with depth and a constant coefficient of variation. To facilitate comparison with the stability number N in Fig.5, Fig. 6 shows the reliability R, as a function of the depth ratio D. The results show that as D is increased in the range $1 < D < 2$, R falls quite steeply as might be expected (N is also falling in this range), but R continues to fall at a decreasing rate for $D > 2$.

This further emphasises the nature of the "seeking out" advantages of RFEM. Failure mechanisms will remain within the $D \leq 2$ range for a deterministic slope with $\beta = 15°$ and $M = 2$, but can go into $D > 2$ probabilistically, if weak soil happens to occur in this deeper range.
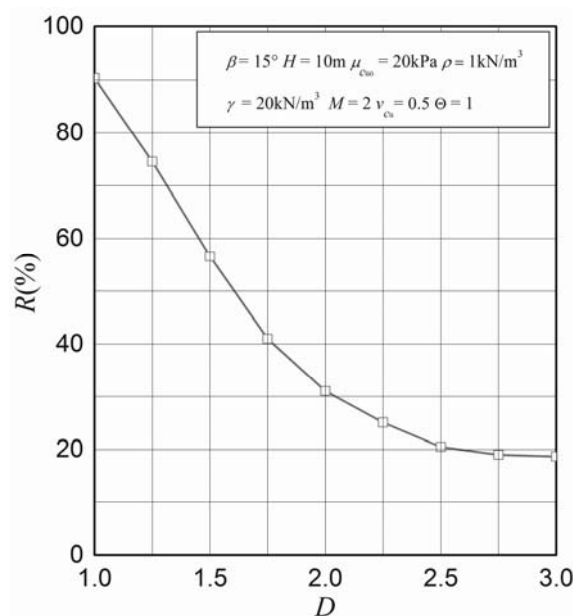
Figure 6. RFEM analyses showing that R ($= 1 - p_f$) continues to fall in the $D > 2$ range

2.3 Random Infinite Slopes

The "seeking out" phenomenon is strikingly demonstrated in the case of a random infinite slope analysis, where a $1 - D$ random field is used to describe the variation of strength properties in the vertical direction. Examples of two random fields, one with "long" and "short"

spatial correlation lengths are shown in Figs. 7(a), 7(b) respectively.

The role of cohesion, friction and pore pressure were considered by Griffiths et al. (2011), but for the purposes of this section, only an undrained infinite slope will be discussed. Deterministically, the factor of safety of an undrained infinite slope of height H and constant strength c_u is given by

$$FS = c_u / (\gamma H \cos\beta \sin\beta) \qquad (7)$$

where β is the slope angle and γ is the saturated unit weight. From Eq. (7), it is clear that the minimum factor of safety occurs at the greatest depth, i.e. when $z = H$. If the soil properties are randomized however, and c_u varies with z as in Fig. 7, failure will occur when the ratio c_u/z is a minimum, which will not necessarily occur at the base. All that is needed for analysis of the random case, is to compute FS from Eq. (7) for each slice in the range $0 < z < H$ and select the minimum value. The analysis is essentially "seeking out" the weakest path through the infinite slope.

Fig. 8 shows the probability of failure (proportion of Monte-Carlo simulations where the minimum $FS < 1$) as a function of the dimensionless spatial correlation length ($\Theta = \theta/H$).

Clearly the smaller correlation length gives more opportunities for failure due to the rapidly varying strength with depth, and therefore the highest probability of failure. Conversely, the "single random variable" solution where $\Theta \to \infty$ is clearly unconservative.

3. Worst Case Spatial Correlation Length

The infinite slope example and results shown in Fig. 8 clearly indicate that the probability of failure is a maximum when the spatial correlation length $\Theta \to 0$. This is a fairly obvious example of a "worst case" spatial correlation length because the system involves a series of elements which fails at the "weakest link" (i.e. where c_u/z is a minimum). In this perfectly brittle system, the smaller the value of Θ, the more likely it is that a weak link will be
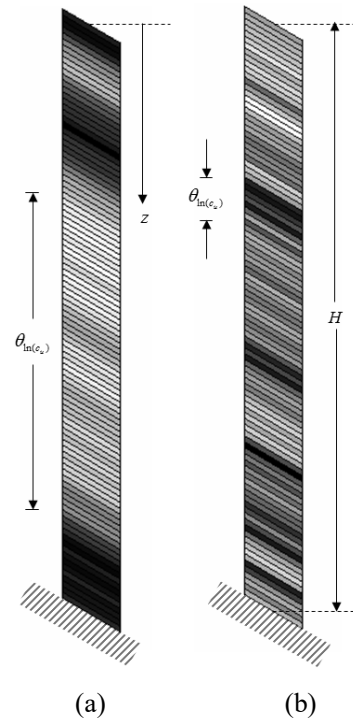
Figure 7. Infinite slope with random shear strength and (a) "long" and (b) "short" spatial correlation lengths
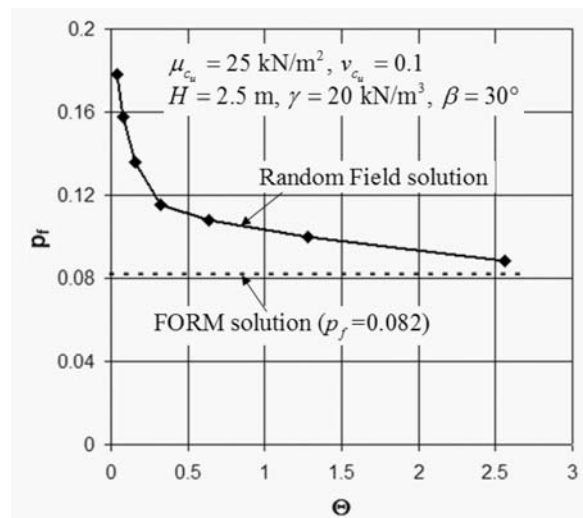
Figure 8. Influence of spatial correlation length on the probability of failure of a random infinite slope

found in the depth range $0 < z \le H$ and the higher the p_f.

Evidence of a "worst case" phenomenon has also been observed in other probabilistic geotechnical analyses, although not always as strikingly as in Fig. 8. Baecher and Ingra (1981)

in a study of foundation settlement, used a stochastic finite element approach to show that the standard deviation of differential settlement between two footings, reached a maximum at a spatial correlation length similar to the footing separation. Griffiths and Fenton (2001) observed a modest reduction in the mean bearing capacity of a footing on an undrained random soil when the correlation length was of the order of the footing width. Examples of "worst case" spatial correlation lengths in foundations and earth pressure analyses have also been reported by the authors.

3.1 Block compressibility

Allahverdizadeh et al. (2015) used RFEM to investigate the influence of spatial correlation length on the compressive strength of a block of unconfined Mohr-Coulomb material with the typical mesh shown in Fig. 9. A similar problem was also considered by Ching et al. (2014).

Assuming lognormal random properties and consistent units with mean values $\mu_{\tan\phi'} = 0.5774$ and $\mu_{c'} = 100$, the "characteristic" mean compressive strength can be given by

$$q_{mean} = 2\mu_{c'} \left[\mu_{\tan\phi'} + \left(1 + \mu_{\tan\phi'}^2\right)^{0.5} \right] = 346.4 \quad (8)$$
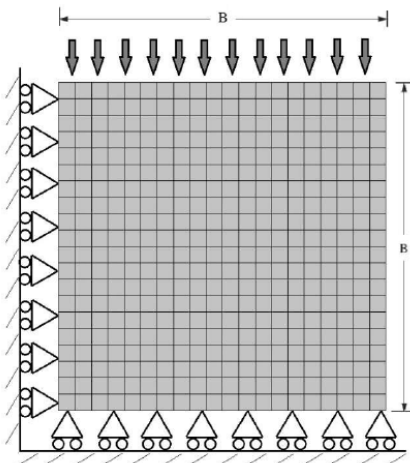
Figure 9. Typical RFEM mesh for compressive strength analysis of a block

Following RFEM and Monte-Carlo simulation, Fig. 10 shows minima in the mean compressive strengths. For the case of

$v = 0.5$ (assuming the same coefficient of variation for both c' and $\tan\phi'$) the reduction is to about 68% of the strength given by Eq. (8) when $\Theta \approx 0.2$. It may be noted that as $\Theta \to 0$, the values tend to a deterministic result based on the median due to finite element local averaging.
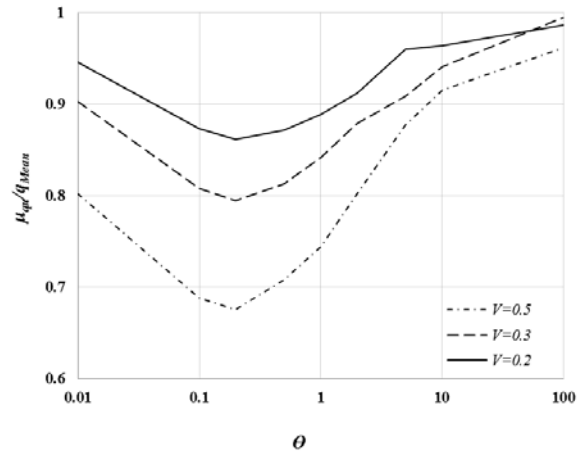
Figure 10. Reduction in mean compressive strength for different values of $\Theta = \theta/B$ and v

A probabilistic interpretation including both the simulated mean and the standard deviation is shown in Fig. 11.
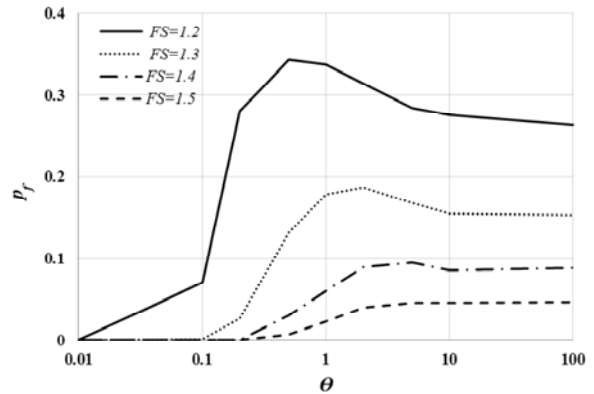
Figure 11. Probability of failure defined as
$$p_f = P\left[q_{ult} < q_{mean}/FS\right]$$

The most pronounced maxima in p_f occur at lower factors of safety and intermediate values of $\Theta \approx 1$. It seems that the optimal spatial correlation lengths facilitate the formation of failure mechanisms through the block and hence push up the probability of failure.

3.2 Slope stability

"Worst case" spatial correlation lengths can also be observed for some slope stability analysis. Fig. 12 shows three FE meshes corresponding to different slopes consisting of undrained clay.
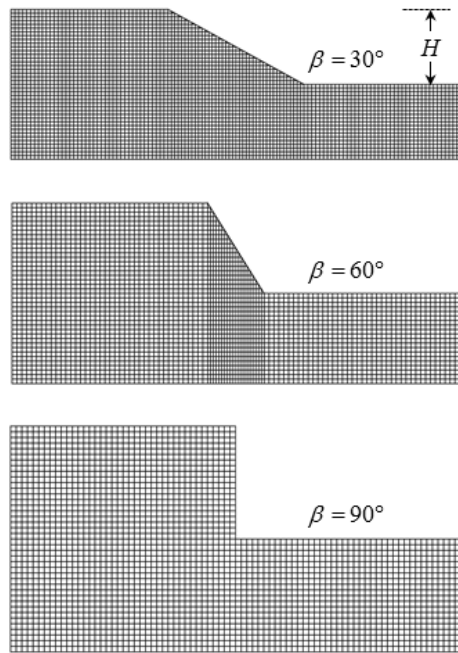
Figure 12. Meshes used in RFEM slope analyses

Two sets of RFEM results for these slopes with stationary lognormal random fields are shown in Figs. 13(a),(b) which have been deliberately chosen to highlight the "worst case" phenomenon. All *FS* values are based on the mean strength. Fig. 13(a) shows the results for three different slopes with a fixed mean strength and coefficient of variation as indicated. Fig.13(b) also varies the mean strength.

The $\beta = 90°$ result in both figures is the same. The coefficient of variation is fixed at $v_{c_u} = 0.5$ since this is often considered to be a practical upper bound for variability of undrained strength (e.g., Lee et al. 1983; Phoon and Kulhawy 1999). The most pronounced maxima in Fig. 13b occur when the mean factor of safety is quite low. i.e. $FS \approx 1.15-1.32$ and when the spatial correlation length is in the range $0.1 < \Theta < 0.5$.
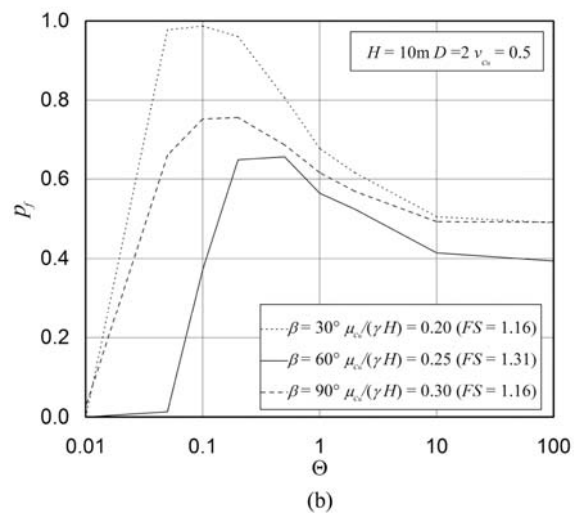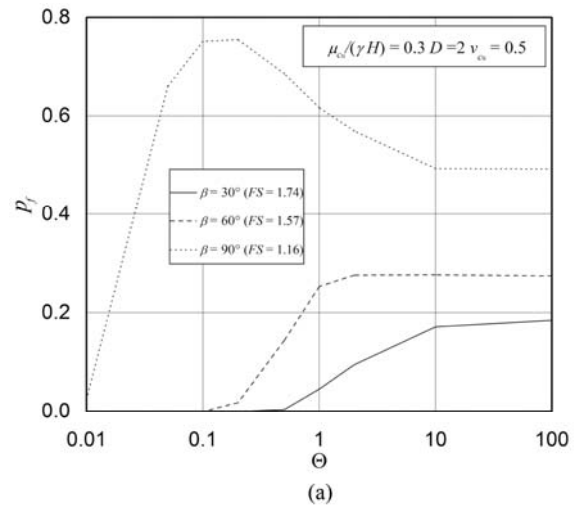
Figure 13. Examples of "worst case" spatial correlation lengths in RFEM analysis of slopes with different angles and strengths

Consideration of extreme values of Θ is useful for validation. When $\Theta \rightarrow 0$, the slope become deterministic, with a uniform strength fixed at the median of the lognormal pdf. In all cases shown in Fig. 13, the median corresponds to FS > 1, so $p_f = 0$.

When $\Theta \rightarrow \infty$, each Monte-Carlo simulation generates a different uniform strength, and p_f is simply the proportion of simulations where the mean $FS < 1$. The $\Theta \rightarrow \infty$ case has an analytical solution which was presented as a chart by Griffiths and Fenton (2004) using the formula

$$p_f = \Phi\left[\frac{\ln(1+v_{c_u}^2) - 2\ln(FS)}{2\sqrt{\ln(1+v_{c_u}^2)}}\right] \qquad (9)$$

where $\Phi[.]$ is the standard normal cumulative distribution function. Griffiths and Fenton (2004) noted that this chart, reproduced here as Fig. 14, could be unconservative for relatively low mean factors of safety and relatively high coefficients of variation.

As an example, when the mean $FS = 1.31$ and $v_{c_u} = 0.5$, the probability of failure from the chart is given as $p_f \approx 0.37$, which is the asymptote towards which the $\beta = 60°$ result is heading in Fig. 13b. Clearly $\Theta \to \infty$ in this case leads to an unconservative result.
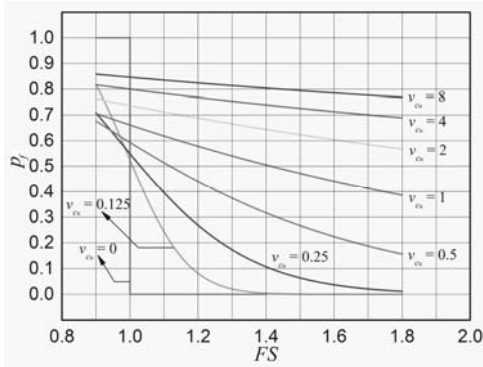
Figure 14. Mean *FS* vs. *pf* assuming infinite spatial correlation ($\Theta \to \infty$) for undrained clays (after Griffiths and Fenton 2004)

A further example demonstrating the contrast between the Griffiths and Fenton (2004) chart and an RFEM analysis is shown in Fig. 15. The actual dimensions used in the RFEM analyses are shown on the figure. The chart result ($\Theta \to \infty$) with $v_{c_u} = 0.5$ is shown as a smooth line and the RFEM results corresponding to several different spatial correlation lengths are also displayed. It can be seen that the lower values of Θ give conservative results (higher *pf* values) towards the left side of the figure, corresponding to lower mean *FS* values. It may be noted that the highest spatial correlation length considered in Fig. 15, $\Theta=5$, is becoming parallel to the $\Theta \to \infty$ line, so the cross-over point is more sensitive to natural fluctuations caused by the Monte-Carlo process

(the results presented in Fig. 15 used 2000 simulations).
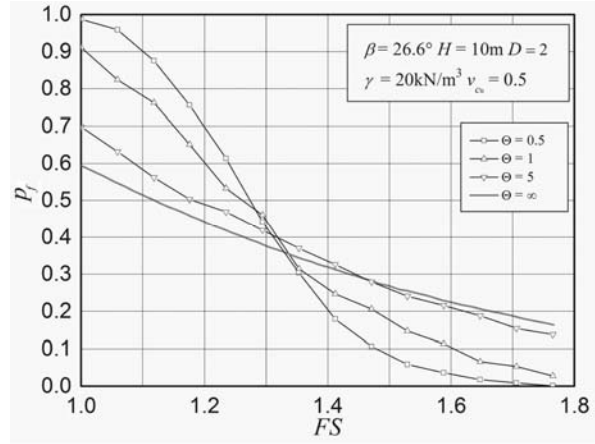
Figure 15. Influence of spatial correlation by RFEM compared with chart results from Fig.14

Even without spatial variability, a further problem with Fig. 14 as noted by Griffiths and Fenton (2004) is that the use of the mean *FS* leads to unrealistically high probabilities of failure (e.g., note the variation of *FS* with *pf* for the case of $v_{c_u} = 0.5$). Clearly, the choice of the mean strength to calculate the *FS* is overly optimistic in this case.

A more detailed discussion of the choice of the characteristic values for computation of *FS* was presented in Griffiths and Fenton (2004). Great care should be taken when attempting to make direct comparisons between factors of safety and probabilities of failure There are well-known counter-intuitive examples (e.g., Lacasse et al. 2013a) in which a given slope can, at the same time, have a higher factor of safety and a higher probability of failure than a second slope!

4. A note on input distribution types
Hicks and Samy (2002) reported RFEM results on undrained slopes exhibiting both uniform and linearly increasing "Gibson soil" random field distributions. Those authors commented on the convenience of the normal distribution, but also the well-known disadvantage that the distribution can lead to "impossible" negative values.

Fig. 16 shows a typical slope failure analysis in which unacceptable negative strength

values have crept into an RFEM analysis by the use of an unmodified normal distribution. Even though very few elements may become negative, the numerical effects can be locally spectacular, even though the rest of the analysis appear to be performing normally.
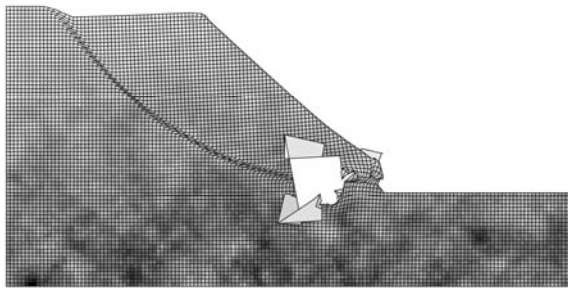
Figure 16. Influence of a negative soil strength on the slope stability analysis of a random soil

Hicks and Samy (2002) went on to note that the inevitable negative values that come with a normal distribution can be easily rectified for low and intermediate values of v_{c_u} by introducing a lower bound on c_u. For a normal distribution, 99.73% of data lie in the range, $\mu_{c_{uz}} \pm 3\sigma_{c_{uz}}$, hence for $v_{c_u} < 0.33$, the exclusion of any values less than $\mu_{c_{uz}} - 3\sigma_{c_{uz}}$ will result in only 0.135% of data being truncated. Although this is a small proportion, if a mesh with several thousand elements, such as that shown in Fig. 16, is being used, it is likely that several elements will become negative in every simulation, especially for smaller values of Θ. In a slope stability problem dominated by low strength elements, this truncation will certainly influence the computed p_f.

In order to investigate this, a slope with a stationary random field was analysed using (i) a lognormal distribution, and (ii) a truncated normal distribution in which simulations including one or more elements with properties falling below a threshold defined by $c_{zi} < \mu_{cz} - \alpha\sigma_{cz}$ were truncated from the analysis. The influence of α is shown in Fig. 17.

As might be expected, increasing α results in increasing p_f, because fewer low-strength (positive) elements are being excluded. Results
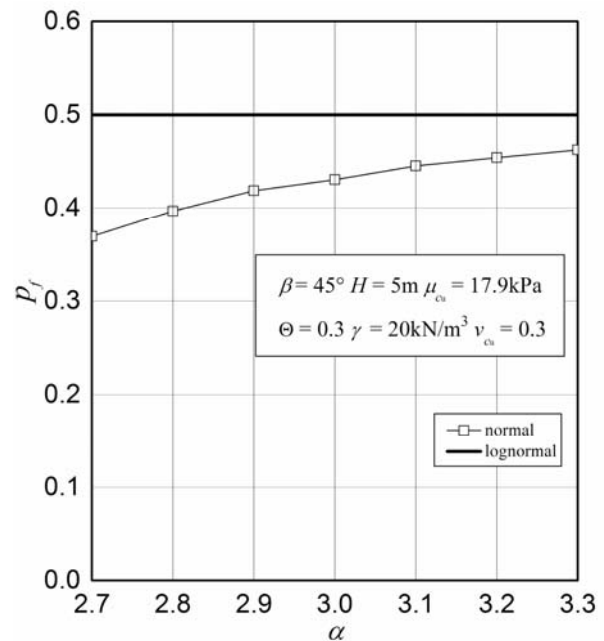
Figure 17. Comparison of lognormal and truncated normal distributions in RFEM

in which any simulation which included a negative which included a negative property were excluded gave essentially the same result as $\alpha = 3.3$. Results from the truncated normal distribution as α increases, seem to be slowly heading towards the lognormal result of $p_f \approx 0.5$.

4.1 The bounded tanh distribution
The lognormal distribution remains the authors' preferred distribution on account of its simple transformational relationship with the normal distribution, and its non-negative character. The distribution is skewed however, and can deliver very high values in the right tail. The possibility of high values may be not an issue in a geotechnical stability or deformation problem, where occasionally high strengths or stiffnesses may be encountered. It is not reasonable however, to use lognormal to model properties which are physically bounded (e.g., the friction angle, Poisson's ratio etc.). For example, if the friction angle ϕ' of a sand is to be made random, (as opposed to the preferred $\tan\phi'$), it might reasonably be bounded in the range $28° < \phi' < 48°$ (e.g., Bardet 1997). Neither normal nor lognormal distributions would be suitable for such a range, in which case the

bounded "tanh distribution" becomes an attractive option. The shape of the tanh distribution has considerable flexibility via two curve fitting parameters, but the simplest version is one that is symmetrical about its mid-point, and has the appearance of a normal distribution with its tails anchored to the "$x-\text{axis}$". Such a tanh distribution for a generic random variable X, bounded in the interval (a,b), is given by the pdf

$$f_X(x) = \frac{\sqrt{\pi}(b-a)}{\sqrt{2}s(x-a)(b-x)} \bullet \exp\left\{-\frac{1}{2s^2}\left[\pi \ln\left(\frac{x-a}{b-x}\right)\right]^2\right\}$$

$$\text{(10)}$$

with the following parameters

$$\mu_X = \frac{1}{2}(a+b), \quad \sigma_X \approx \frac{0.46(b-a)s}{\sqrt{4\pi^2+s^2}}$$

$$\text{(11)}$$
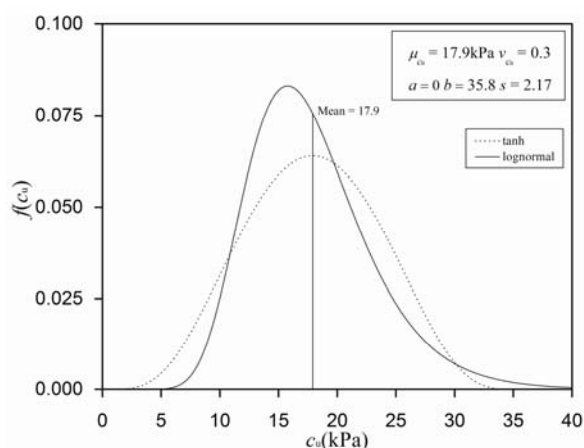
Figure 18. Comparison of the bounded tanh and lognormal distributions

The bounded tanh distribution can be shown to be a simple transformation of a normally distributed random variable (see Fenton and Griffiths 2008 for more details). The pdf given by Eq. (10) and the corresponding lognormal distribution with the same mean and standard deviation from Eq. (11) are plotted together in Fig. 18.

The results of RFEM analyses using these two distributions are shown in Fig. 19, and are clearly similar, with the tanh distribution giving a slightly more pronounced "worst case" probability. The authors feel that further RFEM

probabilistic studies in geotechnical engineering using the tanh distribution would be of value.
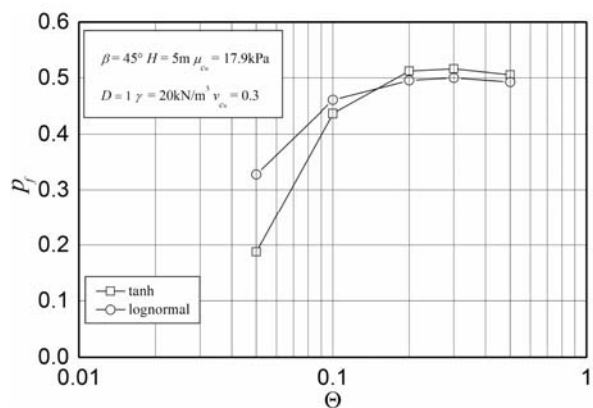
Figure 19. RFEM slope analysis using bounded tanh and lognormal distributions

5. Concluding Remarks

In 1997, Lane and Griffiths wrote a paper entitled, "Finite element slope stability analysis. Why are engineers still drawing circles?" That paper was entirely focused on deterministic slope stability analysis, however that question needs to be asked with even greater urgency when it comes to probabilistic slope stability analysis.

As shown in this paper and elsewhere, if a slope consists of spatially variable soil, the critical failure mechanism will "seek out" the weakest path through the soil which will not necessarily be circular. Only FE (or FD) slope stability methodologies allow the failure mechanism to form "naturally", without any assumptions being imposed *a priori* by the choice of slope stability method. For this reason, classical limit equilibrium methods should be avoided in probabilistic slope stability analysis. The imposition of an incorrectly shaped failure mechanism (e.g., circular) will typically deliver an "upper bound" (unconservative) solution.

The paper has also discussed the phenomenon of the "worst case" correlation length. This is the correlation length that leads to the *highest* probability of failure with all other parameters held constant. This was demonstrated through examples of infinite slopes, block compressibility and simple slope stability analyses. It was shown that the "worst

case" correlation length is problem dependent. Infinite slopes gave a "worst case" at very short correlation length ($\Theta \to 0$). Typical slopes with higher probabilities of failure displayed a "worst case" at intermediate correlation lengths, while those with smaller probabilities of failure displayed a "worst case" at higher values ($\Theta \to \infty$).

A brief discussion was introduced about the random distribution type assumed for shear strength in a probabilistic slope stability analysis. The normal distribution remains popular on account of its simplicity and familiarity, however it brings with it an inevitable possibility of generating negative properties which are physically meaningless. Negative values are easily excluded from an analysis, however this raises theoretical questions since the truncated normal is not a known distribution with an analytical basis. The authors' preference is usually to use the lognormal distribution for modelling geotechnical parameters, on account of its non-negativity and its simple relationship to the normal. For bounded properties however, such as the friction angle or Poisson's ratio, the "tanh distribution" is an attractive alternative worthy of further investigation.

Appendix

Given that for any random variable X with lognormal distribution

$$\sigma_{\ln X} = \sqrt{\ln\left(1 + v_X^2\right)} \qquad (A1)$$

$$\mu_{\ln X} = \ln \mu_X - \sigma_{\ln X}^2/2 \qquad (A2)$$

Since v_{c_u} is constant

$$\sigma_{\ln c_{zi}} = \sigma_{\ln c_{0i}} \qquad (A3)$$

The relationship between c_{zi} and c_{0i} is therefore

$$c_{zi} = \exp\left(\frac{\ln c_{0i} - \mu_{\ln c_{0i}}}{\sigma_{\ln c_{0i}}} \times \sigma_{\ln c_{zi}} + \mu_{\ln c_{zi}}\right)$$

$$= \exp\left(\frac{\ln c_{0i} - \mu_{\ln c_{0i}}}{\sigma_{\ln c_{0i}}} \times \sigma_{\ln c_{0i}} + \mu_{\ln c_{zi}}\right)$$

$$= \exp\left(\ln c_{0i} - \mu_{\ln c_{0i}} + \mu_{\ln c_{zi}}\right)$$

$$= \exp\left(\ln c_{0i} - \mu_{\ln c_{0i}} + \ln \mu_{c_{zi}} - \frac{1}{2}\sigma_{\ln c_{zi}}^2\right)$$

$$= \exp\left(\ln c_{0i} - \mu_{\ln c_{0i}} + \ln \mu_{c_{zi}} - \frac{1}{2}\sigma_{\ln c_{0i}}^2\right)$$

$$= \exp\left(\ln c_{0i} - \ln \mu_{c_{0i}} + \ln \mu_{c_{zi}}\right)$$

$$= c_{0i}\frac{\mu_{c_{zi}}}{\mu_{c_{0i}}} \qquad (A4)$$

According to Eq. (1), $\mu_{c_{zi}} = \mu_{c_{uH}} - \rho(H - z)$. As the mean of initial values c_{0i} is $\mu_{c_{uH}}$, $\mu_{c_{0i}} = \mu_{c_{uH}}$, thus

$$c_{zi} = c_{0i}\frac{\mu_{c_{uH}} - \rho(H - z)}{\mu_{c_{uH}}} \qquad (A5)$$

Notation

a	lower bound of the interval
b	upper bound of the interval
B	width and height of a block
c'	effective cohesion
c_{0i}	initial strength values
c_u	undrained strength
c_{zi}	strength values after adjustment
D	depth ratio
H	slope height
H_0	height above crest where $c_u = 0$
i	simple counter
M	strength gradient parameter
FS	factor of safety
n	number of elements
N	stability number
p_f	probability of failure
q_{mean}	mean compressive strength
q_{ult}	ultimate compressive strength
R	reliability ($= 1 - p_f$)
s	scale parameter

v_X	coefficient of variation of X
X	generic random variable
z	depth below crest
α	standard deviation factor
β	slope angle
γ	unit weight
$\Phi[.]$	standard normal cumulative distribution function
Θ	dimensionless spatial correlation length
θ	spatial correlation length
$\theta_{\ln(c_u)}$	spatial correlation length of $\ln(c_u)$
μ_X	mean value of X
ρ	strength gradient
σ_X	standard deviation of X
ϕ'	effective friction angle
ϕ_u	total stress friction angle (=0)

References

Allahverdizadeh, P., Griffiths, D.V. and Fenton, G.A. 2015. Influence of soil shear strength spatial variability on the compressive strength of a block. *Georisk* (Online)

Alonso, E.E. 1976. Risk analysis of slopes and its application to slopes in Canadian sensitive clays. *Géotechnique*, 26(3): 453-472.

Baecher, G.B. and Christian, J.T. 2003. *Reliability and Statistics in Geotechnical Engineering*. John Wiley & Sons, Hoboken, NJ.

Baecher, G.B. and Ingra, T.S. 1981. Stochastic FEM in settlement predictions. *Journal of the Geotechnical Engineering Division, ASCE*, 107(4): 449-463.

Bardet, J-P. 1997. *Experimental Soil Mechanics*. Prentice-Hall Inc., New Jersey.

Ching, J., Phoon, K.-K. and Kao, P.-H. 2014. Mean and variance of mobilized shear strength for spatially variable soils under uniform stress states. *Journal of Engineering Mechanics*, 140(3): 487-501.

Christian, J.T., Ladd, C.C. and Baecher G.B. 1994. Reliability applied to slope stability analysis. *Journal of Geotechnical Engineering, ASCE*, 120(12): 2180-2207.

Duncan, J.M. 2000. Factors of safety and reliability in geotechnical engineering. *Journal of Geotechnical and Geoenvironmental Engineering*, 126(4): 307-316.

EI-Ramly, H., Morgenstern, N.R. and Cruden, D.M. 2002. Probabilistic slope stability analysis for practice. *Canadian Geotechnical Journal*, 39(3): 665-683.

Fenton G.A. and Griffiths, D.V. 2008. *Risk Assessment in Geotechnical Engineering*. John Wiley & Sons, Hoboken, NJ.

Fenton G.A. and Vanmarcke, E.H. 1990. Simulation of random fields via local average subdivision. *Journal of Engineering Mechanics*, 116(8): 1733-1749.

Fenton, G.A. and Griffiths, D.V. 1993. Statistics of block conductivity through a simple bounded stochastic medium. *Water Resour Res*, vol.29, no.6, pp.1825-1830.

Fenton, G.A., Griffiths, D.V. and Urquart, A. 2003. A slope stability model for spatially random soils. In *Proc ICASP9*, (eds. A. Der Kiureghian et al.), Pub. Millpress, Rotterdam, Netherlands, pp. 1263- 1269.

Gibson, R.E. and Morgenstern, N. 1962. A note on the stability of cuttings in normally consolidated clay. *Géotechnique*, 12(3): 212-216.

Griffiths, D.V. and Fenton, G.A. 1993. Seepage beneath water retaining structures founded on spatially random soil. *Géotechnique*, 43, no.4, pp.577-587.

Griffiths, D.V. and Fenton, G.A. 2000. Influence of soil strength spatial variability on the stability of an undrained clay slope by finite elements. In *Slope Stability 2000*. Edited by Griffiths, D.V. et al, ASCE, GSP No. 101, pp. 184-193.

Griffiths, D.V. and Fenton, G.A. 2001. Bearing capacity of spatially random soil: The undrained clay Prandtl problem revisited. *Géotechnique*, 51(4): 351-359.

Griffiths, D.V. and Fenton, G.A. 2004. Probabilistic slope stability analysis by finite elements. *Journal of Geotechnical and Geoenvironmental Engineering*, 130(5): 507-518.

Griffiths, D.V., Huang, J. and Fenton G.A. 2009. Influence of spatial variability on slope

reliability using 2-D random fields. *Journal of Geotechnical and Geoenvironmental Engineering*, 135(10): 1367-1398.

Griffiths, D.V., Huang, J. and Fenton G.A. 2011. Probabilistic infinite slope analysis. *Computers and Geotechnics*, 38(4): 577-584.

Griffiths, D.V., Huang, J. and Fenton G.A. 2015. Probabilistic slope stability analysis using non-stationary random fields. In *5th International Symposium on Geotechnical Safety and Risk*, Rotterdam, pp. 690-695.

Griffiths, D.V. and Lane, P.A. 1999. Slope stability analysis by finite elements. *Géotechnique*, 49(3): 387-403.

Griffiths, D.V. and Yu, X. 2015. Another look at the stability of slopes with linearly increasing undrained strength. *Géotechnique*, 65(10): 824-830.

Hassan, A.M. and Wolff, T.F. 1999. Search algorithm for minimum reliability index of earth slopes. *Journal of Geotechnical and Geoenvironmental Engineering*, 125(4): 301-308.

Hicks, M.A. and Samy, K. 2002. Influence of heterogeneity on undrained clay slope stability. *Quarterly Journal of Engineering Geology and Hydrogeology*, 35: 41-49.

Hunter, J.H. and Schuster, R.L. 1968. Stability of simple cuttings in normally consolidated clay. *Géotechnique*, 18(3): 372-378.

Husein Malkawi, A.I., Hassan, W.F. and Abdulla, F.A. 2000. Uncertainty and reliability analysis applied to slope stability. *Structural Safety*, 22(2): 161-187.

Lacasse S. 1994. Reliability and probabilistic methods. In *13th International Conference on Soil Mechanics and Foundation Engineering*, 1994. New Delhi, India, pp. 225-227.

Lacasse, S. and Nadim, F. 1996. Uncertainties in characterising soil properties. In *Uncertainty in the geologic environment: From theory to practice*. Edited by Shackelford, C.D. et al., ASCE GSP 58, pp. 49-75.

Lacasse, S., Nadim, F., Høeg, K., Liu, Z.Q. and Nadim, F. 2013a. An homage to Wilson Tang: Reliability and risk in geotechnical practice - How Wilson led the way. In *4th International Symposium on Geotechnical Safety and Risk*, Hong Kong, pp. 3-26.

Lacasse, S., Nadim, F., Høeg, K. and Gregersen, O. 2004. Risk assessment in geotechnical engineering: The importance of engineering judgement. In *Advances in Geotechnical Engineering: The Skempton Conference*, Institution of Civil Engineers, pp. 856-867.

Lacasse, S., Nadim, F., Vanneste, M., L'Heureux, J.-S., Forsberg, C.F. and Kvalstad, T.J. 2013b. Case studies of offshore slope stability. ASCE, GSP No. 231, pp. 2379-2418.

Lacasse, S., Nadim, F. and Uzielli, M. 2007. Hazard and risk assessment of landslides. In *Geo-Denver 2007*, ASCE, GSP 157, pp. 1-10.

Lane, P.A. and Griffiths, D.V. 1997. Finite slope stability – Why are engineers still drawing circles? In Proceedings of Numerical Models in Geomechanics, *NUMOG VI*. Edited by Pande, G.N. and Pietruszczak S., Pub, Balkema, pp.589-593.

Lee, I.K., White, W. and Ingles, O.G. 1983. *Geotechnical Engineering*, Pitman, London.

Li, K.S. and Lumb P. 1987. Probabilistic design of slopes. *Canadian Geotechnical Journal*, 24(4): 520-531.

Low, B.K., Gilbert, R.B. and Wright, S.G. 1998. Slope reliability analysis using generalized method of slices. *Journal of Geotechnical and Geoenvironmental Engineering*, 124(4): 350-362.

Lumb, P. 1970. Safety factors and the probability distribution of soil strength. *Canadian Geotechnical Journal*, 7(3): 225-242.

Lumb, P. 1972. Probabilistic aspects of slope stability. In *Proceedings of the First International Symposium on Landslide Control*, Japan, The Japan Landslide Society, pp. 125-131.

Matsuo, M. and Kuroda, K. 1974. Probabilistic approach to the design of embankments. *Soils and Foundations*, 14(1): 1-17.

Mostyn, G.S. and Li, K.S. 1993. Probabilistic slope stability – State of play. In *Probabilistic Method in Geotechnical Engineering: Proceedings of the conference*, Edited by Li, K.S. and Lo, S-C.R., Pub. A.A. Balkema, pp. 89-110.

Mostyn, G.S. and Soo, S. 1992. The effect of autocorrelation on the probability of failure of

slopes. In *6th Australia, New Zealand Conference on Geomechanics: Geotechnical Risk*, pp. 542-546.

Phoon, K.-K. and Kulhawy, F.H. 1999. Characterization of geotechnical variability. *Canadian Geotechnical Journal*, 36(4): 612-624.

Tang, W.H., Yucemen, M.S. and Ang, A.H.S. 1976. Probability-based short term design of slopes. *Canadian Geotechnical Journal*, 13(3): 201-215.

Taylor, D.W. 1937. Stability of earth slopes. *Journal of the Boston Society of Civil Engineers*, 24: 197-246.

Terzaghi, K. 1948. Foreword to the inaugural volume of *Géotechnique*, 1(1).

Uzielli, M., Nadim, F., Lacasse, S. and Kaynia, A.M. 2008. A conceptual framework for quantitative estimation of physical vulnerability to landslides. *Engineering Geology*, 102(3-4): 251-256.

Vanmarcke, E.H. 1977a. Probabilistic modeling of soil profiles. *Journal of Geotechnical Engineering, ASCE*, 103(11): 1227-1246.

Vanmarcke, E.H. 1977b. Reliability of earth slopes. *Journal of Geotechnical Engineering, ASCE*, 103(11): 1247–1265.

Whitman, R.V. 1984. Evaluating calculated risk in geotechnical engineering. *Journal of Geotechnical Engineering, ASCE*, 110(2): 143-188.

Wolff, T.F. 1996. Probabilistic slope stability in theory and practice. In *Uncertainty in the geologic environment: From theory to practice*, Edited by Shackelford, C.D. et al., ASCE, GSP 58, pp. 419-433.

Wong, F.S. 1985. Slope reliability and response surface method. *Journal of Geotechnical Engineering, ASCE*, 111(1): 32-53.

Yong, R.N., Alonso, E., Tabba, M.M. and Fransham, P.B. 1977. Application of risk analysis to the prediction of slope instability. *Canadian Geotechnical Journal*, 14(4): 540-553.